ELSEVIER

Catena 45 (2001) 185–207

CATENA

www.elsevier.com/locate/catena

Runoff and soil erosion under rainfall simulation of Andisols from the Ecuadorian *Páramo*: effect of tillage and burning

Jérôme Poulenard [a,b,*], Pascal Podwojewski [b], Jean-Louis Janeau [c], Jean Collinet [d]

[a] *Centre de Pédologie Biologique (CNRS), 17, rue ND des pauvres, BP 5, 54501 Vandoeuvre les Nancy, France*
[b] *IRD 32, Av. H. Varagnat 93143, Bondy, France*
[c] *IRD IBSRAM-MSEC, Project. P.O. Box 9-109, Jatujak, Bangkok 10900, Thailand*
[d] *IRD Tunis, BP 434, 1004 Tunis, El Menzah, Tunisia*

Received 8 November 1999; received in revised form 26 February 2001; accepted 27 March 2001

Abstract

In northern Ecuador, soils of high altitude grasslands (*páramos*) are mainly non-allophanic Andisols developed on Holocenic volcanic ash. These soils have a high water retention capacity and are the "water tank" of central Ecuador. To assess the effect of land use (burning and tillage) on soil hydrodynamic properties, rainfall simulation was conducted at two different sites. At Pichincha near Quito, the simulation was conducted on a recent volcanic ash soil comparing natural, tilled and burned plots. At El Angel, the simulation was conducted on a mature non-allophanic Andisol comparing natural, recently tilled and formerly cultivated plots.

On natural plots, the infiltration rate was very high and sediment loss very low. Results for infiltration rate and runoff indicated that land use change on *páramos* increased runoff flow and reduced saturated hydraulic conductivity. Superficial reorganisation of the soil surfaces occurred on tilled plots at both sites. This crusting process was fast and resulted in surfaces with very low conductivity at Pichincha. The same processes seemed to be slower at El Angel. The soil surface of recent Andisols at Pichincha was prone to crusting whereas the mature Andisol, at El Angel,

* Corresponding author. Centre de Pédologie Biologique (CNRS), 17, rue ND des pauvres, BP 5, 54501 Vandoeuvre les Nancy, France.
E-mail address: poulenard@wanadoo.fr (J. Poulenard).

0341-8162/01/$ - see front matter
PII: S0341-8162(01)00148-5

with a lower bulk density, was compacted when the kinetic energy of raindrops was high. Water repellency occurred after burning at Pichincha and following long natural air drying after tillage in the non-allophanic A horizon at El Angel. Water repellency combined with the low bulk density of soil aggregates explain the intensity of sediment losses in the abandoned soils after cultivation (Bare fallow plots). Erosion occurred in these areas through floating hydrophobic and stable aggregates.

Keywords: Andisols; Runoff; Erosion; Land use change; Water repellency; Ecuador; *Páramo*

1. Introduction

Andisols (Soil Survey Staff, 1999) generally show a strong resistance to water erosion (Warkentin, 1985; Shoji et al., 1993). This low erodibility is strongly related with the specific physical properties of Andisols: high porosity permits a rapid rainfall infiltration and high structural stability of volcanic ash aggregates (Maeda and Soma, 1985; Nanzyo et al., 1993). However, this behaviour of volcanic ash soils does not completely agree with the field behaviour of lands with Andisols, especially when they are intensively cropped or overgrazed (Pla Sentis, 1992; Van Wambeke, 1992). Various studies have demonstrated the occurrence of high soil losses in Andisols (Raunet, 1991; Warkentin, 1992; Nishimura et al., 1993) particularly after drying of the soil surface.

For many authors, either the hydrodynamic and erosive behaviour on undisturbed Andisols, either the change of these properties after drying, are due to the presence of non-crystalline materials formed by ash weathering. There is abundant literature about the physical properties of Andisols dominated by short range ordered minerals (allophanes and imogolite) (Maeda et al., 1977; Albrook, 1983; Rousseaux and Warkentin, 1976) but little is known about the physical properties and the hydrodynamic behaviour of non-allophanic Andisols dominated by organo-metallic complexes. However, such non-allophanic Andisols cover extensive areas, especially in volcanic tropical mountains where the climate favours organic-matter accumulation (Van Wambeke, 1992).

In the northern and equatorial Andes, the soils of the natural neotropical alpine grasslands (3500–4500 m a.s.l.), the *páramos*, are mainly non-allophanic Andisols (Poulenard, 2000). Very few people live in this high altitude ecosystem, but growing population pressure, together with agrarian reform, have led Andean peasants to increasing use this fragile ecosystem increasingly for agricultural production (De Noni and Viennot, 1993). Typical land use includes, firstly, the use of *páramos* as extensive grassland and to provide fresh and palatable grasses for sheep, the tussock grass layer are burned before introduction of sheep. Once the lower *páramos* has been grazed, farmers often till the soil to grow potatoes. Some authors suggest that burning, tilling or grazing may have major effects on the hydric and erosive properties of the *páramos* (Guhl, 1968; Parsons, 1982; Smith and Young, 1987) but no specific study has been carried out to quantify the impact of land use on the hydrodynamic properties of *páramos* soils. The main aim of this present study was to analyse the impact of farming on the erosive and hydrological characteristics of two different non-allophanic Andisols of the *páramos*.

3 ex envoyé à Quito par Podwo

2. Materials and methods

2.1. Environmental conditions in the páramos

Páramos are the natural neotropical alpine grasslands which occur in the northern and Equatorial Andes of Venezuela, Colombia and Ecuador. They are usually located above the forest line (3200–3600 m a.s.l.) and below the snow line (4500–5000 m a.s.l.). *Páramos* are generally cold and humid, with daily average temperatures ranging between 0°C and 12°C, with little annual variation. Temperature varies greatly between night and day, from below 0°C to 25°C, respectively. Annual precipitation ranges between 1500 and 2000 mm with frequent fog and drizzle. The vegetation of the *páramos* covers about 90% of the soil surface and is dominated by a tussock grass layer associated with acaulescent rosettes.

2.2. Soil genesis in the páramos

The pedological cover of Northern Ecuadorian *páramos* is composed of volcanic ash soils. The soil parent materials are mainly andesitic ashes, which are younger than 10,000 years B.P. The wet and cold climatic conditions of the *páramos* belt (udic to perudic soil moisture regime and isomesic to isocryic soil temperature regime; Soil Survey Staff, 1999) have led to the formation of non-allophanic Andisols (Shoji et al., 1993). Ash glass weathering intensity is controlled mainly by the size and the age of the ashes, as recently reported by Poulenard (2000). Low weathered Andisols, rich in primary minerals (mainly volcanic glasses), are developed on the recent an coarse ashes occurring on the slopes of numerous active volcanoes (Site no. 1, Pichincha). In contrast, Andisols rich in both non-allophanic poorly ordered constituents and associated organic matter (more than 15% of organic carbon) are developed on the oldest and finest ash deposits (Site no. 2, El Angel), (Poulenard, 2000).

2.3. Selected sites: soils, vegetation and land use

Two sites have been selected to represent these two major pedological occurrences. The first site (Pichincha site: PIC) is located at 4000 m a.s.l. on the Pichincha Volcano, close to the city of Quito (Fig. 1); the topsoil developed on the < 300 years B.P. andesitic ashes of the Pichincha Volcano (Hall and Mothes, 1993). The presence of a buried A horizon below a non-weathered lapilli layer has led to the classification of this young Andisol as a Glassy Isomesic Thaptic Hapludand (Soil Survey Staff, 1999). The Pichincha Andisol is characterized by low amounts of amorphous constituents, estimated by oxalate extractable aluminium (Alo) and iron (Feo) (Alo + 1/2 Feo < 2%), a sandy texture and a relatively high bulk density (Table 1).

The second site (El Angel site: GEL) was located at 3600 m a.s.l. near the city of El Angel, in the province of Carchi, Northern Ecuador (Fig. 1) and the ultimate ash deposits are approximatively 3000 years B.P. The soil (Amorphic Isomesic Hydric

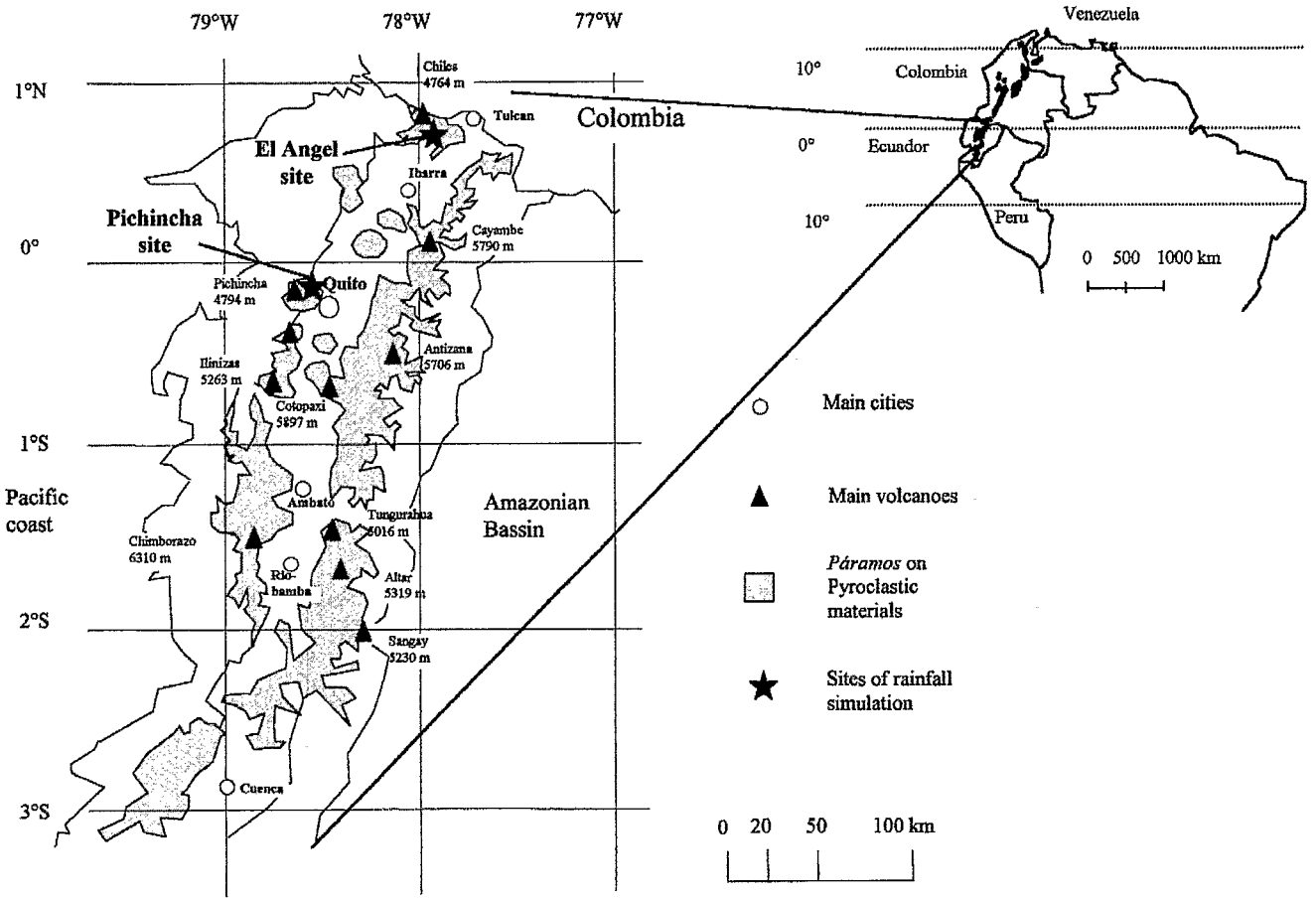

Fig. 1. Localisation of *páramos* in South America and Ecuador; sites of rainfall simulation.

Table 1
Main soil characteristics of the selected undisturbed Pichincha and El Angel Andisols

	Depth (cm)	Org. C[a] (g kg^{-1})	Alo + 1/2 Feo[b] (g 100 g^{-1})	Alp/Alo[c]	Ret-P[d] (g 100 g^{-1})	Glass content[e] (%)	Water retention at −1500 kPa (g kg^{-1})	Bulk density (g cm^{-3})	Total porosity (cm^3 cm^{-3})	Grain size distribution[f] (g 100 g^{-1})			Soil classification (Soil Survey Staff, 1999)
										Sand	Silt	Clay	
Pichincha													
A1	0–20	125	0.52	–	51	28	520	0.8	66	67	28	5	Thaptic Hapludand
A2	20–40	40	1.05	0.72	41	28	270	0.9	64	49	43	8	
2 A3	40–55	27	2.30	0.21	67	46	360	0.7	72	53	40	7	
El Angel													
A1	0–30	212	1.40	0.96	90	42	970	0.4	80	9	65	26	Hydric Pachic Melanudand
A2	30–85	92	3.06	0.41	90	37	590	0.6	73	25	58	17	
Ab1	85–140	150	2.92	0.88	95	49	920	0.4	80	33	51	16	

[a]Org. C = Organic Carbon.
[b]Alo and Feo = ammonium oxalate extractable Al and Fe, respectively.
[c]Alp = pyrophosphate extractable Al.
[d]Ret-P = phosphate retention.
[e]Glass content in the 0.02–2 mm fration.

Pachic Melanudand, Soil Survey Staff, 1999) is rich in silt, clay and organic carbon. It is also characterized by a proeminent melanic epipedon (black, with melanic index < 1.7) (Honna et al., 1988) and by a high water content value of more than 700 g kg^{-1} for a matrix potential value of -1500 kPa (Table 1). In the topsoil, the high amount of organic carbon and the value of the oxalate/pyrophosphate extractable aluminium ratio (Alo/Alp) of nearly 1 suggest the predominance of Al-organic complexes (Table 1). The amount of allophanes, computed following Parfitt and Wilson (1985), is related to the clay content and varies from 40 to 60 g kg^{-1} (Table 1).

The vegetation at Pichincha, consists of a predominant tussock grass layer (*Stipa* sp., *Calamagrostis* sp. and *Agrostis* sp.) and is associated with small plants (mainly *Lachemilla orbiculata*) occurring between the tussocks, without a bare soil surface. At El Angel, the tussock grass is associated with giant rosette (*Espeletia Asteraceae*), with bare soil surface (nearly 20%) located between tussock grass and giant rosette. This vegetation is typical of the highly humid *páramos*, also found in Colombia and Venezuela.

Finally, the two selected sites are subjected to different types of recent land use. Burning before grazing is the main recent land use at Pichincha whereas either potato cultivation or mainly bare fallow were the recent land uses occurring at the lower altitudes of the El Angel site. The weak phosphorus availability at the El Angel Andisols only allows one or two cultivations of potato leading to large areas of *páramos* under permanent bare fallows. Gully erosion has not been reported on the surfaces of the selected undisturbed *páramo* sites whereas sheet erosion occurs on their cultivated *páramos* surface counterparts.

2.4. Water retention, water repellency and water-stable aggregates

Water retention by drainage was determined on A_1 and A_2 non-cultivated soil cores equilibrated at matrix potential values of 10 kPa following the plate method (Klute, 1986) (four replicates per soil sample). Topsoil samples of soil surface from both sites were kept in wet conditions or dried at 30°C for 48 h and analysed as follows. First, water repellency was measured on both wet and 30°C air-dried soils following the capillary rise method (Michel, 1998) which allows the computation of the mean apparent contact angle between water and solid: pore interfaces (three replicates per soil sample). Second, the mean proportion of water-stable > 200 μm aggregates was also determined on both wet and 30°C air-dried soils following the procedure described by Bartoli et al. (1991) (three replicates per soil sample).

2.5. Simulated rainfall experiments

Simulated rainfall experiments were carried out on plot replicates (surface area of 1 m^2) and of equal slope value (20°). A 2×3 factorial design with three plot replicates for each treatment and four successive rainfalls for each plot was used. The factors were: soil type (the Pichincha and the El Angel Andisols) and treatment (three per site).

Treatments were applied to the surrounding surface areas of 10 m^2 and were selected according to the main type of land use in each region: natural conditions plots, standard tillage plots (10-cm topsoil was tilled manually), burned plots (Pichincha) and bare fallow plots which had been used for a single potato cultivation (El Angel). For this last treatment, the potatoes were harvested 3 months before the rainfall simulation experiments leading to a dry and bare topsoil. A sprinkling infiltrometer was used to simulate rainfall with kinetic energies similar to natural rainfall of the same intensities (Asseline and Valentin, 1978). Four successive simulated rainfalls were carried out in each plot replicate, as follows. The time between two successive rainfall events was 3, 12 and 24 h for the first, the second and the third runs, respectively. Each rainfall event occurred during 90 min and comprised six successive sub-runs with increasing rainfall intensity values (Table 2). Kinetic energy of the rainfall events was calculated using the classical equation: $E = (210 + 89\log I)D$, where E is the kinetic energy, I the rainfall intensity and D the rain depth of the rainfall event (Morin, 1996). Although little is known about the natural rainfall intensities occurring in the *páramos* we selected successive simulated rainfall intensities of cumulated volume of 95 mm for both testing soil response to critical rainfall conditions and evaluating the potential effect of land use on the hydraulic and erosive properties of the *páramo* ecosystems.

For modelling, the classical model of runoff and infiltration partition during a rainfall event with constant rainfall intensity (Lafforgue and Naah, 1976) was used, as follows. First, the pre-runoff rainfall volume (PRR) was defined as the cumulative volume of rainfall, in mm, recorded before the runoff occurrence. Second, the infiltration flow was determined as the difference between controlled rainfall intensity and recorded runoff rate. Third, the runoff coefficient (R_c) was computed as the ratio between cumulative runoff lamina and total rainfall depth (D) (95 mm). The pre-runoff rainfall volume and the runoff coefficient indicate the velocity of runoff initiation and production, respectively.

The steady-state infiltration rate (fc) recorded during the permanent regime stage was also linearly related to the rainfall intensity (I), as follows: $\mathrm{fc} = \alpha I + \beta$.

According to Lafforgue and Naah (1976) increase or decrease of the steady-stage infiltration rate as a function of rainfall intensity may be interpreted as follows. Positive

Table 2
Experimental procedure for each run

Sub run	Rainfall intensity ($mm\ h^{-1}$)	Duration (min)	Cumulated rainfall (mm)	Kinetic energy ($J\ m^{-2}$)
1	20	15	5	118
2	27	15	6.75	168
3	50	15	12.5	340
4	70	15	17.5	499
5	90	15	22.5	663
6	120	15	30	918
Total	–	90	95.25	2706

α slope values were attributed to occurrence of soil surface with a high roughness and where the conductivity was heterogeneous: high in the higher positions and lower in hollows (Dunne et al., 1991). In this case, when runoff lamina increases, the proportion of pores accessible for water infiltration (connected macroporosity) increases and the infiltration rate becomes higher. In contrast, negative α slope values were attributed to the development of a relatively impermeable crust or to the reduction of structural porosity (e.g., Valentin, 1991; Nishimura et al., 1993).

The initial saturated hydraulic conductivity (K_s) of the soil surface was assumed to be highly similar to the minimum rainfall intensity necessary for runoff to occur during wet conditions. This threshold was determined as the point where the function $fc = f(I)$ intercepts the first bisectrix (Collinet and Valentin, 1982; Valentin, 1991).

Topsoil samples were collected at 0–20 cm before each rainfall event to determine their water contents and their pore water saturation ratios.

Runoff soil suspensions were also sampled at time intervals depending on runoff rates and analysed thereafter (soil suspension concentration, sediment discharge rate and total soil loss).

2.6. Microrelief measurements and roughness index

The elevation (h) of 361 (19×19) points of each plot was measured before the first and after the fourth rainfall events using an equipment similar to Bielders et al. (1996). Elevation measurements of the points belonging to the edges of the frame were not used because of the edge effects. A three-dimensional model of the soil surface was carried out using the GOCAD package. The standard deviation of the mean elevation value $\sigma(h)$ of each plot replicate, corrected from the general slope effect was calculated and used as a soil surface roughness index. The surface type of each point was also described according to the crust classification of Casenave and Valentin (1992).

3. Results and discussion

3.1. Water retention, water repellency and water-stable aggregates

Water retention curves (Fig. 2) clearly showed that the amount of retained water was very high from 10 up to 200 kPa for both Andisols, which has been reported widely (e.g., Nanzyo et al., 1993). Table 1 (total porosity) and Fig. 1 demonstrate that porosity was saturated at lower matrix potentials. This was attributed to microporosity where capillary forces arise. More porous was the soil sample (see Table 1) richer in retained water it was (Fig. 2).

The water retention curve shows large amounts of water retained at high matrix potentials and demonstrates the predominance of micropores ($R_c < 0{,}1$ μm) for both soils. This pore size distribution is a classical feature of Andisols (Nanzyo et al., 1993).

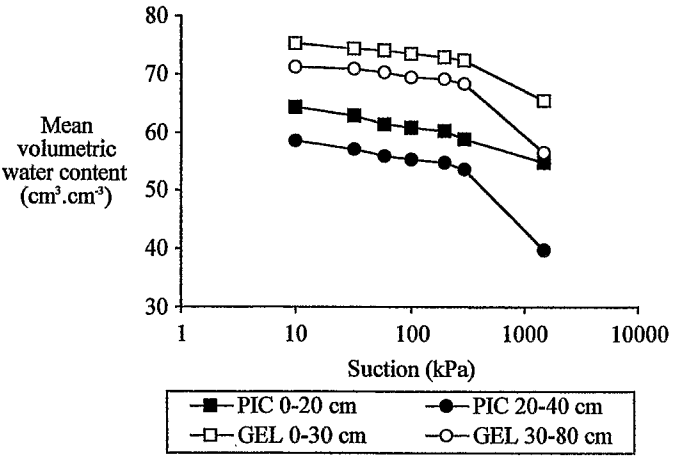

Fig. 2. Water retention curves for the A1 and A2 horizons of Pichincha (PIC) and El Angel (GEL) soils.

These results show also the low amounts of large pores useful for water transmission. The El Angel topsoil present higher microporosity but the amounts of pores with a radius of > 5 μm determined as the difference between total porosity and 33 kPa water retention is very low and almost similar in both cases (4% and 6% for Pichincha and El Angel, respectively). The mean apparent contact angle of wet topsoils, which was mainly attributed to soil structure (capillary pressure), was lower for the Pichincha wet topsoil than for the El Angel wet topsoil counterpart (Table 3).

When the two selected topsoils dried they became both very hydrophobic (Table 3) with contact angle near 90°. Development of water repellency after air-drying is a classical behaviour of peats (Boelter, 1969; Valat et al., 1991) but has been rarely reported for organic-rich Andisols. Water repellency is a function of the type of soil organic matter (Capriel et al., 1995), mainly through the distribution of the polar and non-polar sites of humic polymers (Michel, 1998). According to Valat et al. (1991), in the drying process, polar groups associated with Al and Fe play a major role in the development of water repellency. Then, the development of water repellency in the case

Table 3
Mean water contact angle (CV = 0.5–4%) determined by capillary rise and mean water stable aggregates (CV = 5–10%) on the wet and the dried Pichincha (PIC) and El Angel (GEL) undisturbed topsoils

Site	Horizons	Depth (cm)	Water contact angle (°)		Water stable aggregates (g 100 g^{-1})	
			Field moisture	Dried 48 h at 30°C	Field moisture	Dried 48 h at 30°C
PIC	A1	0–20	52.5	87	38.6	57
GEL	A1	0–30	69	85	62.5	91

of non-allophanic Andisols could be linked with the presence of aluminium and iron-humus complexes.

Finally, the proportion of water-stable aggregates was higher for the El Angel topsoil, which is very rich in organic matter, than its Pichincha topsoil counterpart, independent of the hydric status of the soils (Table 3). Water-stable aggregate stability was attributed to the binding effect of organic matter (Table 1). When the selected topsoils were air-dried at 30°C for 48 h, very strong shrinkage occurred leading to compact structures with porosity values of less than 0.5 cm^3 cm^{-3} for site topsoils. Conversely, the proportion of water-stable aggregates became very high (Table 3) but the same opposition between the two selected topsoils always occurred, which validated our hypothesis of the binding effect due to organic matter.

3.2. *Pre-runoff rainfall volume and runoff coefficient*

For the different treatments, the mean runoff coefficients (R_c) and the mean pre-runoff rainfall volumes (PRR), and their variabilities, were plotted as a function of successive rainfall events (Fig. 3). The results were as follows.

(A) Major change occurred between the first and the second simulated rainfall with an increase of R_c and, conversely, a decrease of PRR, both less pronounced for the two undisturbed topsoils. R_c and PRR values were nearly constant for the next rainfall events, independent of the soil treatment. This dynamic was less pronounced for the two undisturbed topsoils. This was attributed to the fact that the selected topsoils were not saturated. We validated this hypothesis by showing that the mean pre-runoff rainfall volume occurring on *undisturbed plots* decreased as a function of the initial pore water saturation (Fig. 4). Initial water saturation for the fourth run (after 24 h without rainfall) is equivalent to the initial condition before the first rainfall event for the Pichincha site. Antecedent rainfall volume and time between events are clearly the key point of the pre-runoff rainfall. At El Angel, the variations of pore water saturation are lower because of their high values. The effect of time between each event is clearly lower. These results suggested that the resilience time of the soil to recover the status previous to the rainfall events is lower for the young non-allophanic Andisol than for the mature one.

(B) Runoff was the key process in the anthropic topsoils (runoff coefficient of 60–75% for the third last simulated rainfall events) whereas 80–90% of the simulated rainfall infiltrated in the natural topsoils (Fig. 3). Results of both PRR and R_c parameters therefore indicated that the recent land use of the *páramos* produced a drastic change of hydrodynamic behaviour of the topsoils by increasing the velocity of both runoff initiation and flow, whatever the site and the treatment. This was mostly attributed to the crust development on the anthropic topsoil surfaces whereas no crusts were observed on their undisturbed topsoil surface counterparts.

(C) PRR and R_c were much higher for the anthropic Pichincha topsoils than for their El Angel topsoil counterparts (Fig. 3). This was attributed to steady-stage infiltration rate variabilities which were also higher for the anthropic Pichnicha topsoils than for their El Angel topsoil counterparts (Fig. 3).

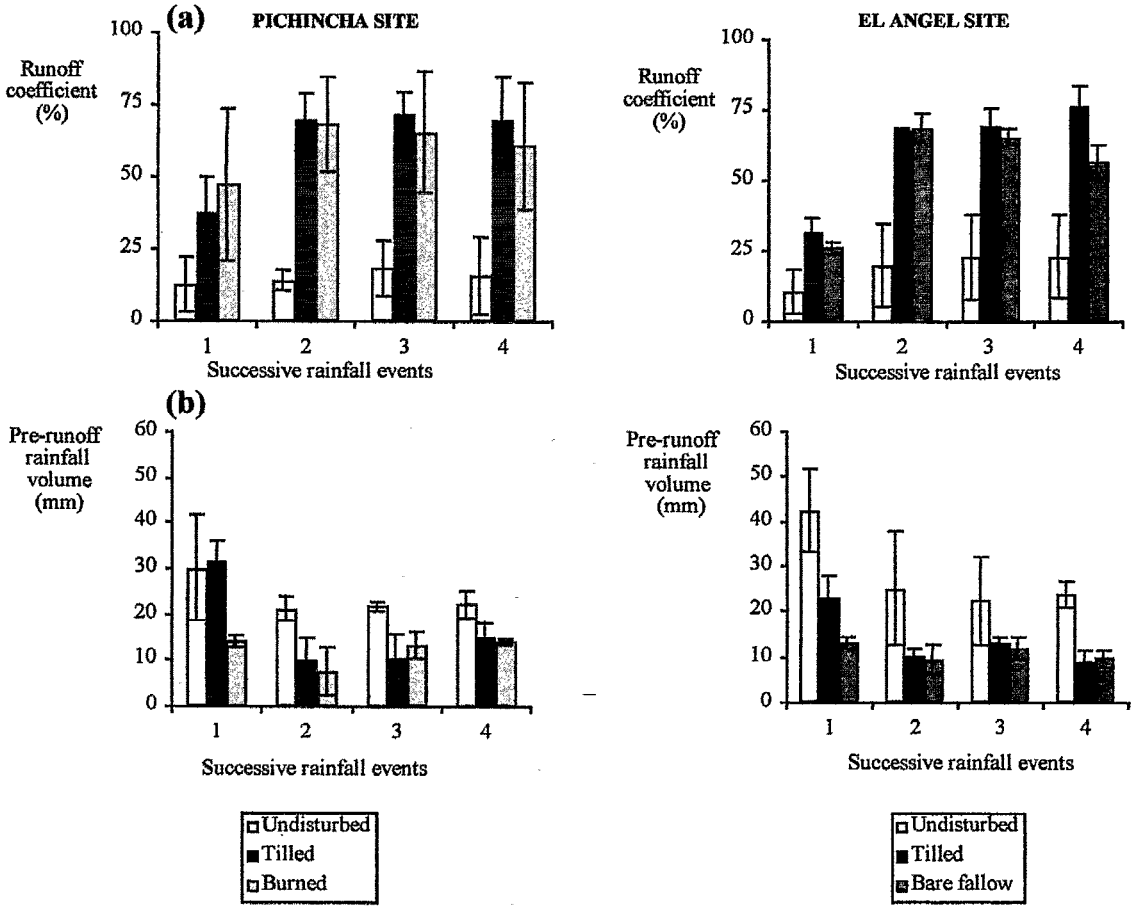

Fig. 3. Evolution of the mean runoff coefficient (a) and of the mean pre-runoff rainfall volume (b) as a function of successive rainfall events for different soil surface treatments.

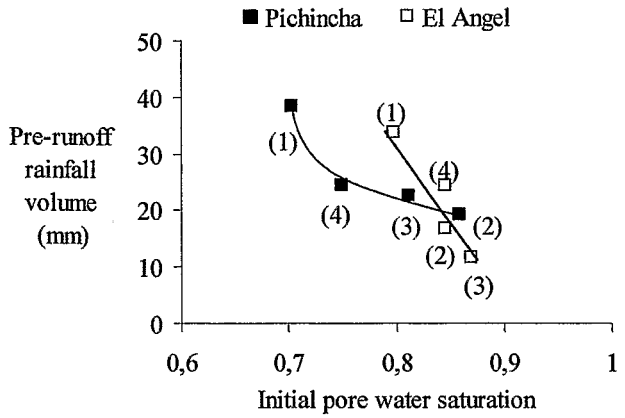

Fig. 4. Examples of pre-runoff rainfall volume as a function of initial pore water saturation for the Pichincha and El Angel undisturbed topsoils during the successive four rainfall events. Order of the rainfall events are enclosed in parenthesis.

(D) Soils dried very highly by fire (burned plots from Pichincha) or through long air exposure without soil cover (bare fallow plots from El Angel) showed significant lower pre-runoff rainfall for the first run (Fig. 3) suggesting lower hydraulic conductivity before the soil crusting process occurred during the first runs.

3.3. Infiltration rates and rainfall intensities

Fig. 5 indicates the evolution of the mean slope α (a) and the mean saturated conductivity K_s (b) as a function of cumulative kinetic energy for the different runs. For the undisturbed plots, this slope is positive and quite constant at both sites showing the lack of crusting process. The steady-stage infiltration rate of the undisturbed topsoils increased (positive α) from the beginning of each simulated rainfall to its end, with a more pronounced effect for the Pichincha topsoil than for its El Angel topsoil counterpart (Fig. 5). It suggests a spatial variation of K_s between the top of the tussocks and the bare microdepressions between tussocks.

The saturated hydraulic conductivity was about 60 mm h^{-1} at the Pichincha site and showed few variations between the different rainfall events. Contrariwise, K_s from the undisturbed El Angel site was significantly higher for the first run (nearly 70 mm h^{-1}) but tended to decrease with the successive runs. This distinctive behaviour between both undisturbed sites is attributed to (i) vegetal cover (% of bare soil) and (ii) pore size distribution (Fig. 2). Our results suggested high water permeability for both undisturbed Andisols, as found by Warkentin (1992) and Nanzyo et al. (1993). However, the water retention curves (Fig. 2) showed a large predominance of microvoids with few pores with radii > 5 μm. Hasegawa (1997) revealed that non-uniform infiltration along preferential flow is a common process under high rainfall intensity for mature Andisol in Japan similar to the *páramos* soils. Despite the absence of cracks and fissures visible at

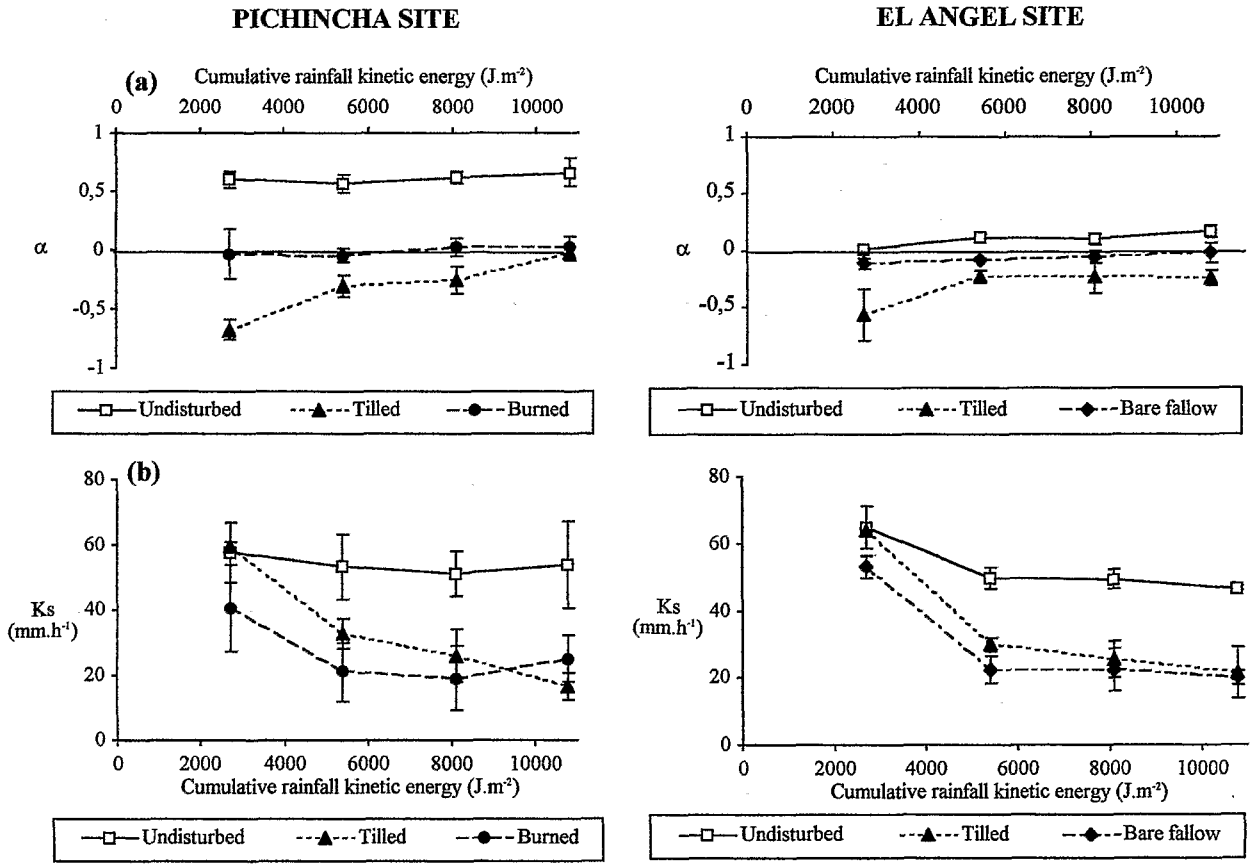

Fig. 5. Evolution of α, the slope of the linear relationship between steady stage infiltration rate and rainfall intensities (a) and K_s, the saturated hydraulic conductivities (b) as a function of cumulative kinetic energy for different soil surface treatments.

the soil surface, preferential flow in biopores and grass root network could explain (i) the increase of infiltration rate with rainfall intensity and (ii) the apparent contradiction between pore size distribution and high hydraulic conductivity.

The tilled plots of both site present a negative slope of the relation $fc = f(I)$, indicating occurrence of the soil crusting process. For the Pichincha site, the coefficient α tended to increase with the successive rainfall events and α was near 0 for the fourth rainfall suggesting that superficial crusting had almost finished. The slope α was low for the first run at El Angel, but significantly higher for the next runs. Stability of the infiltration rate was not reached on this plot. The decrease of K_s was similar at both sites (from > 60 to lower than 20 mm h^{-1}), but the decrease was regular for Pichincha while the main reduction occurred between run 1 and 2 at El Angel.

A similar decrease of the infiltration rate as a function of both cumulative rainfall kinetic energy and crust development has been described previously in either semi-arid tropical sandy soils (e.g., Valentin, 1991) or temperate silty soils (e.g., LeBissonais and Singer, 1992; Mualem et al., 1990). Soil crusting in volcanic ash soils is less known. Andisols present very high structural stability (e.g., Shoji et al., 1993), and are theoretically resistant to the formation of structural crusts. Only few studies have been carried out on seal formation processes in volcanic ash soils and on their effect on topsoil hydraulic properties. Nishimura et al. (1993) showed the occurrence of seal formation on an Andisol topsoil surface which was subjected to simulated rainfall and demonstrated that crust development led to the classical non-linear decrease of the infiltration rate as a function of rainfall duration, as previously reported in tropical sandy and temperate silty cultivated soils. Our study clearly showed that tilled organic-rich Andisols, were affected by soil crusting leading to a non-linear decrease of the infiltration rate (Fig. 5). Moreover, our results suggested that this process should be related to the weathering stage of volcanic ash soils. Structural crust formation in young Andisols was related to aggregate breakdown by the kinetic energy of raindrops. This process results from the relatively low structural stability of aggregates in this young Pichincha Andisol (Table 3). Thus, young Andisols such as at the Pichincha site, with low amounts of secondary constituents, are more susceptible to seal formation than a mature Andisol such as at El Angel, characterized by strong intra-aggregate binding by organic matter (in our case, organo-metallic complexes). However, the mature non-allophanic Andisol appeared more sensitive to the compaction of the soil surface than the young Andisol. This led to the formation on the tilled El Angel soil surfaces of a compacted seal which limited the proportion of large pores which connected the soil surface to its very porous soil structure (bulk density < 0.4 cm^3 g^{-1}).

On burned plots, we observed little variation of slope α of the relation $fc = f(I)$ close to 0. This result suggests an homogeneous plot where K_s is constant during each event. Mean K_s is close to 40 mm h^{-1} (i.e., lower than for undisturbed plots at Pichincha) but the standard variation appears high; K_s tended to decrease between runs 1 and 2 but tended to increase between runs 3 and 4.

Bare fallow plots presented a constant slight negative α coefficient suggesting a light crusting process. However, K_s in the first run was significantly lower than for undisturbed and tilled plots; K_s decreased strongly between runs 1 and 2, and remained quite constant (about 20 mm h^{-1}) for the subsequent runs.

Water repellency occurred after burning on a young Andisol and after natural air drying in the bare fallow plots of a mature non-allophanic A horizon. This water repellency was substantiated by low pre-runoff rainfall in the first run, and hydraulic conductivity lower than the undisturbed plot. Many authors have reported the effect of burning on water repellency and its consequences in different environments (Wells et al., 1979; Imeson et al., 1992). Savage et al. (1972) have shown that the transformation of organic matter products by heating is responsible for water repellency. In the case of a non-allophanic Andisol, very rich in organic matter, water repellency could appear with just natural air drying (see Table 3). On bare fallow plots at El Angel this is evident. Similar evidence of hydrophobic behaviour in bare organic-rich soil with andic properties was recently reported by Clothier et al. (2000). The increase of K_s between runs 3 and 4 for burned plots (Fig. 3) could be attributed to a progressive breakdown of water repellency as it was reported in the same reference (Clothier et al., 2000).

Our results showed that a decrease of the infiltration rate was a consequence of initial water repellency. According to Barrett and Slaymaker (1989) and Dekker and Ritsema (1996), development of preferential flow paths is highly probable in such water repellent soils but our data are unable to substantiate the occurrence of this process.

3.4. Sediment losses and the erosion process

Fig. 6 shows the relation between cumulative soil losses and cumulative kinetic energy. Sediment losses from natural undisturbed *páramos* were very low, with total erosion being less than 100 g (Fig. 6). Sediment losses increase linearly as a function of cumulative rainfall kinetic energy. The slope of the relation could be considered as a soil erodibility index. The burned plots at Pichincha and the tilled plots at El Angel exhibited moderate rates of sediment losses, with total erosion lower than 250 g. For tilled plots at Pichincha we observed a non-linear relationship between erosion and kinetic energy with steep slope increase during the first three runs and a lower increase for the fourth run. The crusting processes in tilled Pichincha plots occurred during the three first runs (see Fig. 5 with a coefficient α near 0 for the fourth run). After crust development, at the fourth rainfall event, runoff was high but lapilli and compact structural crusts protected the surface from erosion. Subsequently, erosion produced by the fourth run was very low. Breakdown of aggregates and splash effect was lower in the case of the recently tilled El Angel site because of the higher structural stability of dried and moist aggregates available (Table 3). Very high organic matter content and classical formation of stable aggregates by drying of the Andisols explained this high stability of structure. As a result, the cumulated erosion was multiplied by a factor of 10 after tillage in Pichincha and by a factor of 5 at El Angel.

Bare plots following fallow at El Angel had very high sediment losses, with a total higher than 1 kg. Erosion was linearly related with kinetic energy with a very high erodibility index. With a coefficient α near 0, this erosion was not related with the crusting process but appeared to be linked with water repellency development. The consequences of water repellency on erosion are documented rarely except on sandy water repellent soil (Dekker and Jungerius, 1990). Our experiments showed very high sediment losses on the hydrophobic cultivated plots of the El Angel soil while Table 3

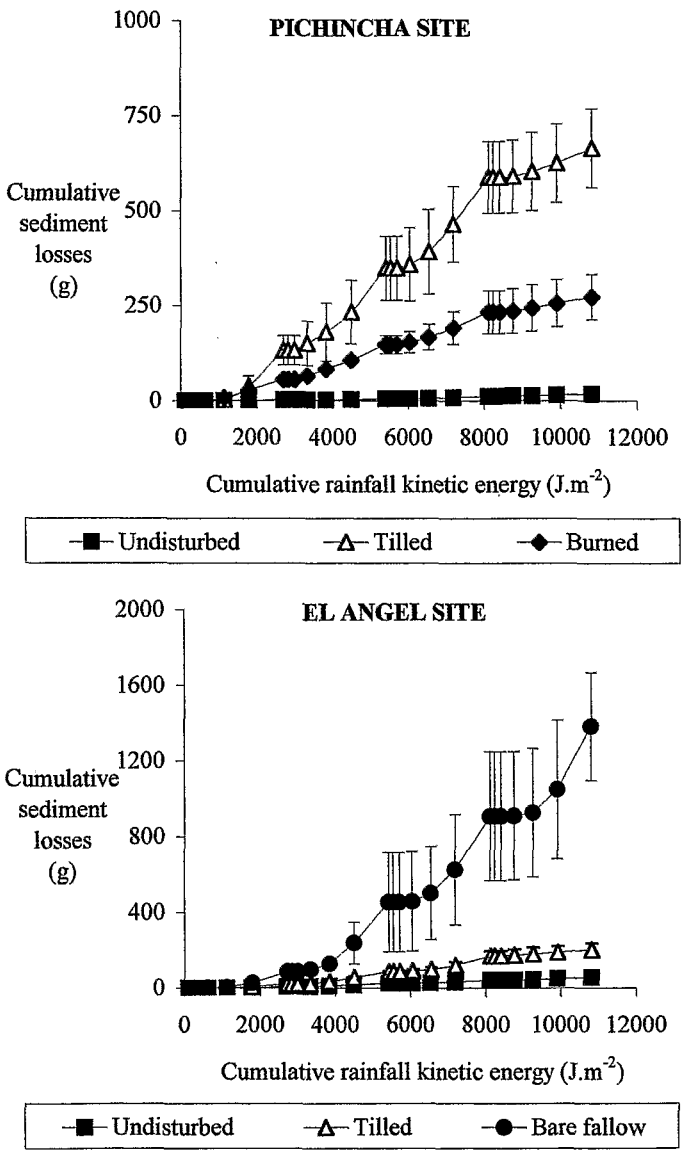

Fig. 6. Evolution of cumulative sediment losses as a function of cumulative kinetic energy for different soil surface treatments.

indicates the very high structural stability of dried aggregates on this soil. These results therefore contradict the classical relation between high stability and low erosion. Water repellency combined with the low bulk density of soil aggregates explains the intensity of sediment losses. Erosion occurred in the form of floating hydrophobic and stable

sand-size aggregates. Similar erosion through floating has been reported for the Andisols of Réunion Island (Raunet, 1991) and Costa Rica (Collinet et al., 1998). Erosion through floating seems to be specific to Andisols where both water repellency and low bulk density are found. On burned *páramos*, the bulk density of the few aggregates detached from the surface appeared to be too high.

3.5. Evolution of soil surface

Table 4 presents the roughness indexes (standard deviation of slope-corrected elevation) before and after the four rainfall events for the plots showing a negative α value (i.e., tilled plots of both site and bare fallow plots). We observed an important decrease in roughness due to rainfall in all cases. The decrease of the roughness index was particularly high for tilled plots and slightly lower for bare fallow plots where the initial roughness was higher (Table 4). Fig. 7 illustrates, for one representative plot of each type, the change in topography before (a) and after (b) the rainfall events. Calculation of the difference between the initial elevation (h_0) and the final elevation (h_f) allows us to draw a map (c) showing the zone of erosion (where $h_0 > h_f$) in red and the zone of accumulation (where $h_0 < h_f$) in blue. This map is superimposed to the initial 3D topography. We show that for tilled plots, redistribution of materials occurred with erosion of the higher parts of the microtopography and accumulation of eroded materials in the micro-depressions (Fig. 7). On bare fallow plots, all the surface was strongly eroded and accumulation was only observed in a local position near the bottom of the plots (and possibly by the edge effect) (Fig. 7). Then, erosion by floating of aggregates led to a total "unstick" of the soil surface as it was yet reported by Raunet (1991).

Table 4
Standard deviation of slope-corrected elevation (σ_h) in cm of the tilled and bare fallow plot replicates before and after the four successive rainfall events.

Replicate	σ_h (cm)	
	Before the rain	After the rain
Pichincha tilled		
1	0.694	0.508
2	0.900	0.536
3	0.740	0.633
El Angel tilled		
1	0.655	0.550
2	0.711	0.632
3	0.789	0.535
El Angel bare fallow		
1	0.943	0.779
2	1.132	0.934
3	1.025	0.846

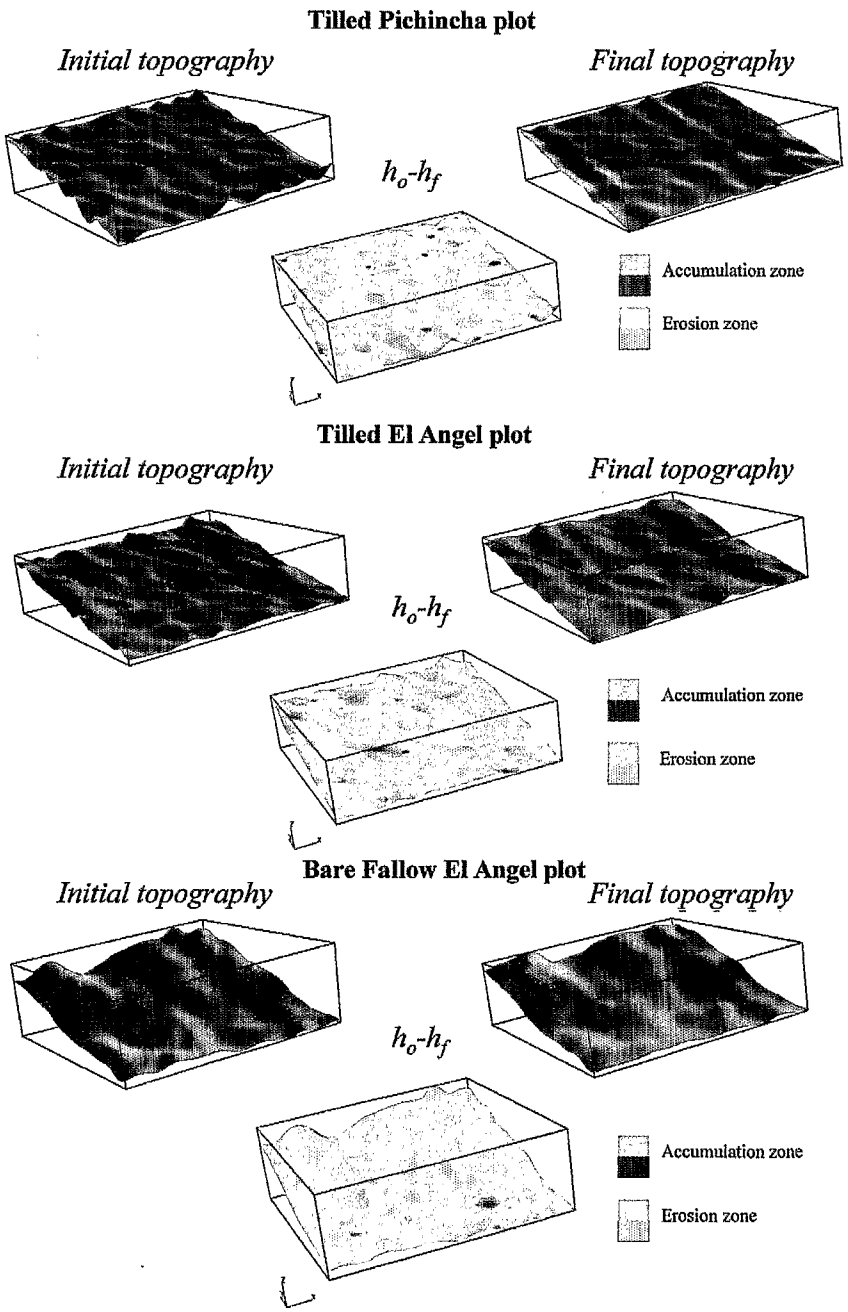

Fig. 7. Examples of initial, final, and differential ($h_0 - h_f$) three-dimensional topographies of 1 m^2 tilled and bare fallow plots before and after the four successive rainfall events.

Before the rainfall experiments, the soil surface of tilled plots was composed at both sites of free aggregates due to tillage (Table 5). After the rainfall, we observed distinctive main features between both sites. On the tilled plots at Pichincha, results indicated the slaking of free aggregates and the formation of (i) a gravel crust and (ii) a structural crust (Table 5). The gravel crust was composed of lapilli remaining on the surface while fine surrounding particles were eroded (see Fig. 8). The structural crust was composed of thin micro-layers of white sands overlaying a finer particle layer where relics of clods disappeared (Fig. 8). This type of crust is similar to the sieving crusts of Valentin and Bresson (1992) (i.e., a sorting of particles reverse to the sedimentary process, where finer materials are found above coarse particles). Near the bottom of the plots, a thin deposit of sand and fine particles formed a depositional crust (Fig. 8). This crust appears to be due to the edge effect of the plot where sedimentation occurred. On the tilled El Angel *páramos*, we observed slaking of free aggregates with a diameter lower than 5 mm. The large surfaces of the plots remained occupied by clods of significant size (> 5 mm) partially included in the matrix bulk soil. We observed also the formation of a plasmic seal (i.e., a thin layer composed of compacted fine materials) which coated the smoothed clods included in the matrix (Fig. 8). This surface type was often associated with depositional crust between the relics of clods. The major process that caused this seal, is the compaction of the soil surface; this limited the amounts of

Table 5
Surface features of the tilled plots replicates before and after the four successive rainfall events
B.R.: before the rain; A.R.: after the rain.

	Vegetation residues (%)	Free aggregates (mm) > 20(%)	> 5(%)	< 5(%)	Lapilli (%)	Structural crust (%)	Depositional crust (%)	Plasmic seal (%)
Pichincha tilled 1								
B.R.	2	9	61	26	2			
A.R	6		3		21	45	4	21
Pichincha tilled 2								
B.R.	0	7	71	20	2			
A.R.	7		1		33	36	3	20
Pichincha tilled 3								
B.R.	0	2	67	27	4			
A.R.	4		1		37	35	8	16
El Angel tilled 1								
B.R.	1	1	44	54				
A.R.	3	3	41	10			1	41
El Angel tilled 2								
B.R.	1	3	50	46				
A.R.	7	1	43	12			1	35
El Angel tilled 3								
B.R.	0	7	57	36				
A.R.	2	1	48	6			2	40

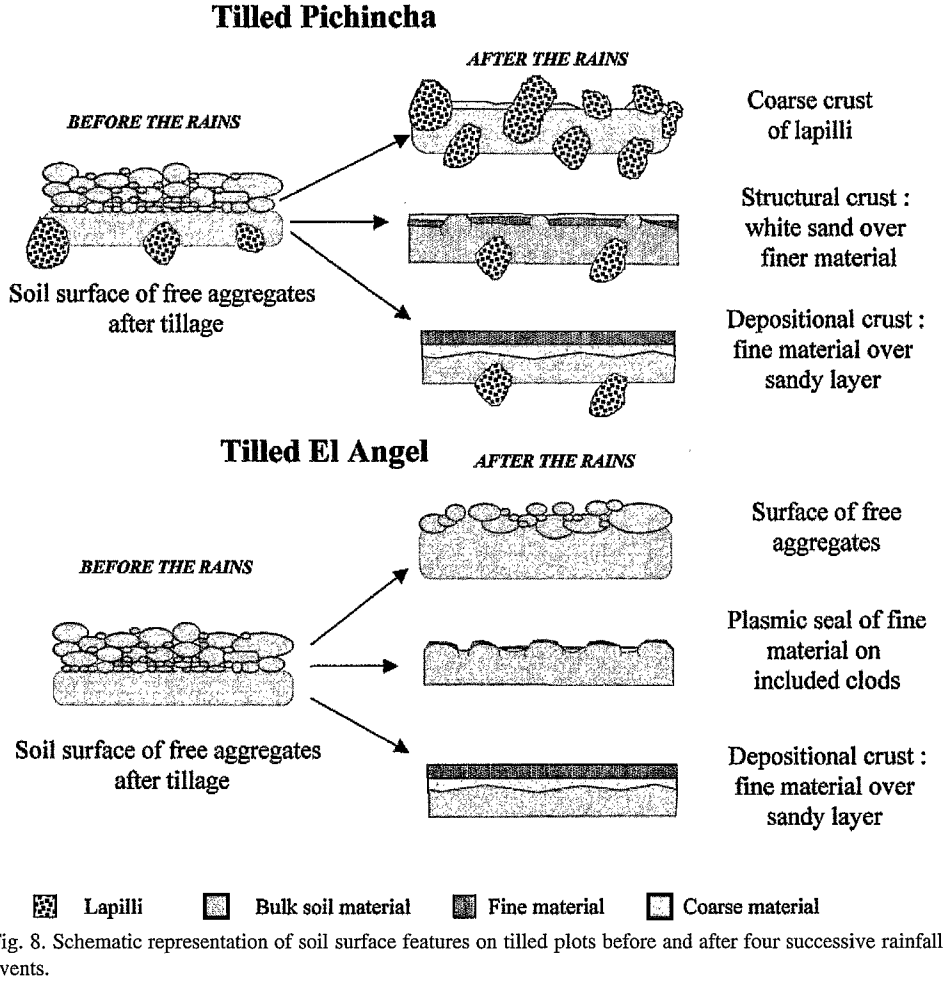

Fig. 8. Schematic representation of soil surface features on tilled plots before and after four successive rainfall events.

large pores connected to the surface of this very porous soil (with bulk density < 0.4) by the energy of the rainfall.

4. Conclusion

1. Land use clearly affects runoff and erosion in the Andean *páramos*. Undisturbed *páramos* present high infiltration and low erosion rates. Both tillage and burning increase the runoff coefficient threefold.

2. Sediment losses increase on all types of land use as compared to undisturbed *páramos* but especially, after land abandonment, the total erosion under our simulated rainfalls increases from approximately 80 g m^{-2} (undisturbed *páramos*) to approxi-

mately 1200 g m^{-2}. This very strong increase is related to floating stable and water-repellent aggregates.

3. After the destruction of the natural vegetal soil cover, the drying of the soil surface due to burning and air-drying seems to be the key factor of the change on hydrodynamic and erosive behaviour.

4. Our results show that the soil characteristics (materials, genesis and weathering stage) have a role in the hydrodynamic behaviour before and after land use change. In the case of non-allophanic Andisols, hydraulic conductivity and its variation over time, water-aggregate stability, soil crusting and the development of hydrophobic properties appear to be strongly related to soil age. Contrary to many hydrological models, the weathering stage and the pedological history of soils need to be accounted for to predict the runoff rate and the intensity of erosion of volcanic ash soil of the *páramos*.

5. Others experiments are required to validate these results for natural rain and at watershed scales. But many field observations confirm that under natural rainfall, the soil crusting process and floating of stable aggregates occurred in the Ecuadorian *páramos* on former cultivated areas.

Acknowledgements

The author thanks Christian Valentin and the reviewers for their improvements of an earlier version of this paper.

References

Albrook, R.F., 1983. Some physical properties of allophane soils from the North Island, New Zealand. N. Z. J. Sci. 26, 481–492.

Asseline, J., Valentin, C., 1978. Construction et mise au point d'un infiltromètre à aspersion. Cah. ORSTOM, Ser. Hydrol. XV (4), 321–349.

Barrett, G., Slaymaker, O., 1989. Identification, characterization and hydrological implications of water repellency in mountain soils, Southern British Columbia. Catena 16, 477–489.

Bartoli, F., Burtin, G., Herbillon, A.J., 1991. Disaggregation and clay dispersion of Oxisols: Na resin, a recommended methodology. Geoderma 49, 301–317.

Bielders, C.L., Baveye, P., Wilding, L.P., Drees, L.R., Valentin, C., 1996. Tillage-induced spatial distribution of surface crusts on a sandy Paleustult from Togo. Soil Sci. Soc. Am. J. 60, 843–855.

Boelter, D.H., 1969. Physical properties of peats as related to degree of decomposition. Soil Sc. Soc. Am. Proc. 28, 433–435.

Capriel, P., Beck, Th., Borchert, H., Gronholz, J., Zachmann, G., 1995. Hydrophobicity of the organic matter in arable soils. Soil Biol. Biochem. 27, 1453–1458.

Casenave, A., Valentin, C., 1992. A runoff capability classification system based on surface features criteria in semi-arid areas of West Africa. J. Hydrol. 130, 231–249.

Clothier, B.E., Vogeler, I., Nagesan, G.N., 2000. The breakdown of water repellency and solute transport through a hydrophobic soil. J. Hydrol. 231–232, 255–264.

Collinet, J., Valentin, C., 1982. Effects of rainfall intensity and soil surface heterogeneity on steady infiltration rate. Proc. 12th Int. Congr. Soil Sci., New Delhi, p. 22.

Collinet, J., Asseline, J., Jimenez, F., Bermudez, A.T., Dromard, S., 1998. Comportements hydrodynamiques et erosifs de sols volcaniques au Costa Rica. Rapport CATIE, Turrialba.

Dekker, L.W., Jungerius, P.D., 1990. Water repellency in the dunes with special reference to Netherlands. Catena Suppl. 18, 173–183.

Dekker, L.W., Ritsema, C.J., 1996. Preferential flow paths in a water repellent clay soil with grass cover. Water Resour. Res. 32, 1239–1249.

De Noni, G., Viennot, M., 1993. Mutations récentes de l'agriculture équatorienne et conséqeunces sur la durabilité des agrosystèmes andins. Cah. ORSTOM, Ser. Pedol. XXVIII (2), 277–288.

Dunne, T., Zhang, W., Aubry, B.F., 1991. Effects of rainfall, vegetation and microtopography on infiltration and runoff. Water Resour. Res. 27, 2271–2285.

Guhl, E., 1968. Los paramos circundantes de la Sabana de Bogota. Su ecologia y su importancia para el regimen hidrologico de la misma. Colloq. Geogr. 9, 195–212.

Hall, M., Mothes, P., 1993. Tefroestratigrafia holocenica de los volcanes principales del valle interandino, Ecuador. Estud. Geogr. 4, 47–67.

Hasegawa, S., 1997. Evaluation of rainfall infiltration characteristics in a volcanic ash soil by time domain reflectrometry method. Hydrol. Earth Syst. Sci. 1 (2), 303–312.

Honna, T., Yamamoto, S., Matsui, K., 1988. A simple procedure to determine melanic index that is useful for differentiating melanic from fulvic Andisols. Pedologist 32, 69–78.

Imeson, A.C., Verstraten, J.M., Mulligen, E.J., Sevink, J., 1992. The effects of fire and water repellency on infiltration and runoff under Mediterranean type forest. Catena 19, 345–361.

Klute, A., 1986. Water retention: laboratory methods. In: Klute, A. (Ed.), Methods of Soil Analysis: Physical and Mineralogical Methods. 2nd edn. American Society of Agronomy, Madison, WI, pp. 635–662.

Lafforgue, A., Naah, E., 1976. Exemple d'analyse expérimentale des facteurs de ruissellement sous pluies simulées. Cah. ORSTOM, Ser. Hydrol. XIII (3), 115–237.

LeBissonais, Y., Singer, M., 1992. Crusting, runoff and erosion response to soil water content and successive rainfalls. Soil Sci. Soc. Am. J. 56, 1898–1903.

Maeda, T., Soma, K., 1985. Classification of Andisols in Japan based on physical properties. International Clay Conference. The Clay Minerals Society, Denver, pp. 174–178.

Maeda, T., Takenaka, H., Warkentin, B.P., 1977. Physical properties of allophane soils. Adv. Agron. 29, 229–264.

Michel, J.C., 1998. Etude de la mouillabilité de matériaux organiques utilisés comme support de culture. PhD thesis, Ecole Nationale Supérieure Agronomique de Rennes, 262 pp.

Morin, J., 1996. Rainfall analysis. In: Agassi, M. (Ed.), Soil Erosion, Conservation and Rehabilitation. Marcel Dekker, New York.

Mualem, Y., Assouline, S., Rohdenburg, H., 1990. Rainfall induced soil seal: (A) A critical review of observations and models. Catena 17, 185–201.

Nanzyo, M., Shoji, S., Dahlgren, R., 1993. Physical characteristics of volcanic ash soils. In: Shoji, S., Dahlgren, R., Nanzyo, M. (Eds.), Volcanic Ash Soils. Genesis, Properties and Utilization. Development in Soil Science, vol. 21, Elsevier, Amsterdam, pp. 189–201.

Nishimura, T., Nakano, M., Miyazaki, T., 1993. Properties of surface crusts of an andisol and their effects on soil-hydrological processes. Catena Suppl. 24, 17–28.

Parfitt, R.L., Wilson, A.D., 1985. Estimation of allophane and halloysite in tree sequences of volcanic soils, New Zealand. In: Caldas, E.F., Yaalon, D.H. (Eds.), Volcanic soils, Weathering and Landscape Relationships of Soils on Tephra and Basalt. Catena Suppl., 7, pp. 1–8.

Parsons, J.J., 1982. The northern Andean environment. Mt. Res. Dev. 2 (3), 253–263.

Pla Sentis, I., 1992. La erodabilidad de los Andisoles en Latino America—tercer panel Latino Americano sobre suelos derivados de cenizas volcánicas. Suelos Ecuat. 22 (1), 33–43.

Poulenard, J., 2000. Les sols des paramos d'Equateur sur couverture pyroclastique: genèse, diversité et propriétés physiques. PhD Thesis, Université de Nancy I, 296 pp.

Raunet, M., 1991. Le milieu physique et les sols de l'île de la Réunion. Conséquences pour la mise en valeur agricole. CIRAD Editions, Montpellier.

Rousseaux, J.M., Warkentin, B.P., 1976. Surface properties and forces holding water in allophane soils. Soil Sci. Soc. Am. J. 40, 446–451.

Savage, S.M., Osborn, J., Letey, J., Heaton, C., 1972. Substances contributing to fire-induced water repellency in soils. Soil. Sci. Soc. Am. Proc. 36, 674–678.

Shoji, S., Dahlgren, R., Nanzyo, M., 1993. Genesis of volcanic ash soils. In: Shoji, S., Dahlgren, R., Nanzyo,

M. (Eds.), Volcanic Ash Soils. Genesis, Properties and Utilization. Development in Soil Science, vol. 21, Elsevier, Amsterdam, pp. 37–70.
Smith, A.P., Young, T.P., 1987. Tropical alpine plant ecology. Annu. Rev. Ecol. Syst. 18, 137–158.
Soil Survey Staff, 1999. Soil Taxonomy. A Basic System of Soil Classification for Making and Interpreting Soil Surveys. 2nd edn. USDA, NRCS, US Gov. Printing Office, Washington, DC.
Valat, B., Jouany, C., Riviere, L.M., 1991. Characterization of the wetting properties of air-dried peats and composts. Soil Sci. 152 (2), 100–107.
Valentin, C., 1991. Surface crusting in two alluvial soils of northern Niger. Geoderma 48, 201–222.
Valentin, C., Bresson, L.M., 1992. Morphology, genesis and classification of surface crusts in loamy and sandy soils. Geoderma 55, 225–245.
Van Wambeke, A., 1992. Soils of the Tropics: Properties and Appraisal. McGraw-Hill, New York.
Warkentin, B.P., 1985. Properties of Andisols important to engineering. VI International Soil Classification Workshop, Chile and Ecuador, Sociedad Chilena de la Ciencia del Suelo. Part I: Papers, pp. 121–150.
Warkentin, R.P., 1992. Manejo de Andisoles relacionado con su estructura. Suelos Ecuat. 22 (1), 9–15.
Wells, C.G., Campell, R.E., Debano, L.F., Lewis, C.E., Frederiksen, R.L., Franklin, E.C., Froelich, R.C., Dunn, P.H., 1979. Effects of fire on soil. A state of knowledge review. General technical Report WO 7.